Equilibrium modeling, kinetic and thermodynamic studies on the adsorption of Cr(VI) using activated carbon derived from matured tea leaves

Mridusmita Goswami · Lukumoni Borah · Debajyoti Mahanta · Prodeep Phukan

Abstract A new porous carbon with high surface area of 1,313.41 $m^2 g^{-1}$ with pore volume 1.359 $cm^3 g^{-1}$ has been synthesized from matured tea leaves by chemical activation method using phosphoric acid. The carbon was found to be highly efficient for removal of Cr(VI) from aqueous solution. The effects of various parameters such as contact time, initial metal ion concentration, pH, temperature and amount of adsorbent on the extent of adsorption were studied. Langmuir, Freundlich and Temkin adsorption models were used to interpret the experimental data. The adsorption data were best fitted with Langmuir isotherm model. The adsorption capacity of Cr(VI) onto the activated carbon calculated from Langmuir isotherm was found to be 30.8 $mg g^{-1}$ at pH 4.8 and temperature 303 K. The adsorption capacity increases from 25.36 to 32.04 $mg g^{-1}$ with an increase in temperature from 303 to 323 K at initial Cr(VI) concentration of 60 $mg L^{-1}$. The adsorption process followed a pseudo second order kinetic model. Thermodynamic parameters ΔH^0 (28.6 KJ mol^{-1}), ΔG^0 at three different temperatures [(−0.145, −1.09, −2.04) KJ mol^{-1}] and ΔS^0 (94.87 J $mol^{-1} K^{-1}$) were calculated. These values confirm the adsorption process to be endothermic and spontaneous in nature.

Keywords Adsorption · Activated carbon · Chemical activation · Isotherms · Kinetics

M. Goswami · L. Borah · D. Mahanta · P. Phukan (✉)
Department of Chemistry, Gauhati University,
Guwahati 781 014, Assam, India
e-mail: pphukan@yahoo.com

1 Introduction

Hexavalent chromium [Cr(VI)] is a major pollutant in water pollution. Due to various industrial activities such as textile dyeing, steel fabrication, leather tanneries, wood preservations, electroplating industries, petroleum refining processes etc., there has been a rapid increase in the amount of Cr(VI)in environment. Naturally, chromium exists in three different oxidation states Cr(II), Cr(III) and Cr(VI) of which Cr(III) and Cr(VI) are stable. Cr(VI) is highly water soluble and has higher mobility than Cr(III) which is the cause of its higher potential to contaminate the ground water. Cr(VI) remains in the form of $HCrO_4^{2-}$, CrO_4^{2-} and $Cr_2O_7^{2-}$ ions in solution and is more toxic than Cr(III) [1, 2]. Cr(VI) is 500 times more toxic than Cr(III) and acute exposure to Cr(VI) causes lung cancer, kidney disease, dermatitis, irritation to eyes and respiratory tracts, gastrointestinal disorders etc. [3]. Therefore, it is necessary to develop an efficient procedure for removal of Cr(VI) from wastewater.

There are several treatment methods that are used for wastewater treatment and recycling [4]. Membrane separation [5], electrocoagulation [6], sedimentation [6], solvent extraction [7], precipitation [6], ion exchange [8], adsorption/filtration [9–11], photocatalytic degradation [12–14] are some of the methods used for treatment of wastewater. Recently, advanced oxidation process (AOP) has also been developed for oxidative degradation of organics in wastewater [15]. Among all these methods, adsorption is the most widely used method because of its operational simplicity and ability to remove both organic as well as inorganic constituents. Use of activated carbon in adsorption method is appreciated as it exhibits high adsorption capacity for pollutants due to high surface area and also due to its nontoxic nature. In recent years, there

has been a continuous search for low cost raw materials for preparation of activated carbon. The focus is mainly given on the utilization of natural plant materials or agricultural waste materials as the precursor of activated carbon [16]. Variety of materials such as sawdust and used tyres carbon [17], cactus, wool, charcoal and pine needles [18], hazelnut shell carbon [19], bottom ash and deoiled soya [20–23], industrial waste and agricultural waste [24, 25] have been reported in the literature for the preparation of adsorbent in wastewater treatment. Carbon nanotube has also been used for the purpose of wastewater treatment [26, 27].

Chemical activation process is more effective than physical activation for the synthesis of activated carbon because of its lower activation temperature and increased yield. Phosphoric acid is widely used as activating agent for chemical activation process as it has many advantages over other activating agents such as potassium hydroxide and zinc chloride etc. [28].

We have recently reported our preliminary results on a new porous carbon prepared from tea precursors [29]. Among three different tea precursors, viz. green tea, black tea, and waste black tea, green tea produced best quality porous carbon [29]. To make this procedure more cost effective, we have carried out a detail study on this particular aspect. In this study, we are reporting the preparation of activated carbon from matured tea (*Camellia Sinensis*) leaves using phosphoric acid as activating agent. In general, matured tea leaves are discarded in tea gardens as it is not useful for production of tea. Moreover, a detail study on Cr(VI) adsorption has also been incorporated in this manuscript. Three kinetic models, pseudo first order, pseudo second order and intra particle diffusion models were used to identify the possible mechanism of the adsorption process. Langmuir, Freundlich and Temkin models were used to analyze the adsorption equilibrium.

2 Experimental

2.1 Materials

The matured tea leaves were collected from a tea garden of upper Assam. The collected materials were cleaned and washed with distilled water to remove the dirt particles. Potassium dichromate and phosphoric acid were obtained from Merck (Mumbai, India). NaOH (Fisher scientific, Mumbai, India) and HCl (Merck, Mumbai, India) were used as received.

2.2 Preparation of the activated carbon

Clean matured tea leaves were boiled in distilled water for several times till the supernatant water became colorless.

The washed material was then dried in oven at 60 °C. This carbon precursor was then grinded, sieved and impregnated with 85 % phosphoric acid and kept in an oven at 100 °C for 3 h. After impregnation the carbon precursor was placed in a temperature programmable tube furnace for thermal treatment. It was heated from room temperature to 500 °C with 1 h holding time at 100 °C interval. Thermal treatment was done under nitrogen atmosphere and the heating rate was fixed at 5 °C min^{-1}. The resulting carbon was washed with 0.1 M HCl and then with distilled water until the washing water was neutral. The resulted activated carbon was then dried, grinded and kept in desiccator for further use.

2.3 Characterization of activated carbon

The surface functional group of matured tea leaves derived activated carbon was characterized by Fourier transform infrared (FT-IR) spectroscopy (Schimadzu, IR affinity) in the range of 4,000–400 cm^{-1}. The crystalline nature of the activated carbon was measured by the powder X-ray diffractometer (Bruker D8 Advance Instrument). The N$_2$ adsorption–desorption isotherm was measured in BET surface area analyzer (Beckmann Coulter SA-3100) at −196 °C for determination of surface area and pore volume etc. Prior to the analysis sample was degassed using helium at 200 °C for 1 h. Surface texture and pore morphology of activated carbon was characterized by scanning electron microscopy (SEM) (LEO 1430VP).

2.4 Adsorption studies

To obtain rate and equilibrium data, the adsorption experiments were carried out in a batch process by using an aqueous solution of Cr(VI). A stock solution of potassium dichromate (1,000 mg L^{-1}) was prepared by dissolving appropriate amount of potassium dichromate in distilled water. Other solutions of desired concentrations were prepared by successive dilution of the stock solution. During the entire experiments we used distilled water of pH 6.8. When required amount of potassium dichromate was added in water pH of the solution became 4.8. In the dissolution process potassium dichromate ionizes as follows:

$$K_2Cr_2O_7 \rightarrow 2K^+ + Cr_2O_7^{2-} \tag{1}$$

$$Cr_2O_7^{2-} + H_2O \rightleftharpoons 2CrO_4^{2-} + 2H^+ \tag{2}$$
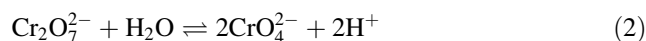
Due to the formation of H$^+$ ions acidity of potassium dichromate solution has been increased. Hence, the pH of the solution decreased to 4.8 and all experiments were performed at this pH. For batch study, 10 mL of Cr(VI) solution of various concentrations (20–100 mg L^{-1}) were taken in 100 mL conical flask and different amount

(1–3 g L^{-1}) of activated carbon was added to it. The mixtures were then agitated in an orbital incubator shaker (Lab Tech, LSI-1005R) at an agitation speed of 120 rpm. The experiments were carried out at different temperatures (303, 313, 323 K) and at different pH (1.5–6). The concentrations of the Cr(VI) at different time intervals were determined by using UV–Visible absorption spectroscopy. The Cr(VI) concentrations were calibrated with Beer-Lambert law at λ_{max} of 352 nm.

3 Result and discussion

3.1 FT-IR analysis

The FTIR spectrum of the activated carbon is shown in Figure (S1, Supporting Information). The absorption band observed at 3,425 cm^{-1} is due to the bonded –OH groups [30], 1,645 cm^{-1} corresponds to COO or C=C groups. The bands around 1,000–1,350 cm^{-1} indicate the existence of C–O single bond in carboxylic acid, alcohols, phenols or esters [31]. The band at 2,920 cm^{-1} is assigned to stretching vibrations of the C–H groups, 1,556 cm^{-1} is an identification of C=O groups [32] and 1,080 cm^{-1} is the C–O stretching vibrations of C–O–C, –OCH$_3$ (indicates lignin structure).

3.2 XRD analysis

The X-ray diffractogram of the activated carbon is shown in Figure (S2, Supporting Information). From the figure it is clear that the nature of the activated carbon is amorphous. The broad peak at 2θ of around 25° corresponding to the (002) plane reflection, reveals the amorphous nature of the activated carbon.

3.3 BET analysis

The surface area of the activated carbon was calculated by BET equation and the t-plot method was used to calculate the micro pore volume and external surface area (mesoporous surface area). Figure (S3, Supporting Information) shows the adsorption desorption isotherm of nitrogen at −196 °C. The total pore volume was determined from the amount of nitrogen adsorbed at a relative pressure close to unity assuming that all the pores were filled with nitrogen at that particular pressure. The graph of adsorption isotherm in Figure (S3, Supporting Information) is a type II isotherm and H4 type hysteresis loop is also observed. H4 hysteresis loop indicates the presence of both micropores and mesopores in the activated carbon. Table 1 shows the physical properties of the prepared activated carbon. From

Table 1 Physical properties of the activated carbon

S_{BET} (m^2 g^{-1})	1313.41
S_{MICRO} (m^2 g^{-1})	294.52
V_{MONO} (cm^3 g^{-1})	295.38
V_{MICRO} (cm^3 g^{-1})	0.119
V_{MESO} (cm^3 g^{-1})	1.239
V_T (cm^3 g^{-1})	1.359

the table it is observed that mesopore volume (V_{MESO}) occupies almost 90 % volume of the total pore volume.

3.4 Morphology study

The SEM image of the prepared activated carbon is shown in Fig. 1. The porous network with well developed pore morphology gives good agreement with the high BET surface area of the activated carbon as shown in Table 1.

3.5 Adsorption study

Adsorption experiments were performed using batch technique and the effect of various parameters on adsorption process was studied.

The percentage removal of Cr(VI) was calculated using the following equation.

$$\% \, \text{Removal} = \frac{(C_0 - C_e)}{C_0} \times 100 \tag{3}$$

The maximum metal ion uptake q_e (mg g^{-1}) was determined as follows:

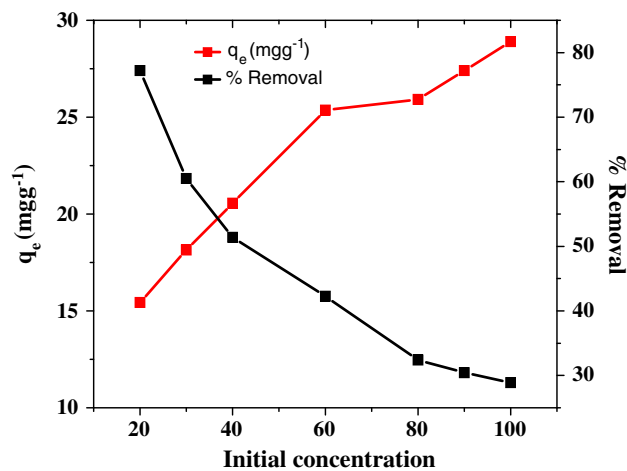$$q_e = \frac{(C_0 - C_e)V}{W} \tag{4}$$

where C_0 and C_e are the initial and final concentration of the Cr(VI) solution (mg L^{-1}) respectively. V is the volume of the solution (L) and W is the mass of adsorbent (g).

3.5.1 Effect of initial metal ion concentration

To study the effect of initial metal ion concentration, the adsorption experiment was carried out by varying the initial metal concentrations from 20 to 100 mg L^{-1}. The amount of adsorbent used was kept fix at 1 g L^{-1}. The effect of initial metal concentration on percentage removal of Cr(VI) and amount of maximum metal ion uptake (q_e) on the activated carbon is shown in Fig. 2. With increase in concentration of Cr(VI) from 20 to 100 mg L^{-1}, the percentage removal of the metal decreases from 77.21 to 28.89 %. This is because of increase in the number of Cr(VI) ions for a fixed amount of adsorbent. On the other hand maximum metal ion uptake of activated carbon increases from 15.4 to 28.8 mg g^{-1} with the increase in the
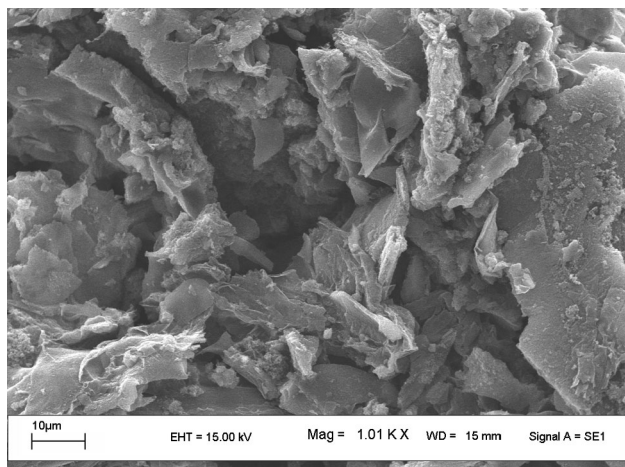
Fig. 1 SEM micrograph of the activated carbon

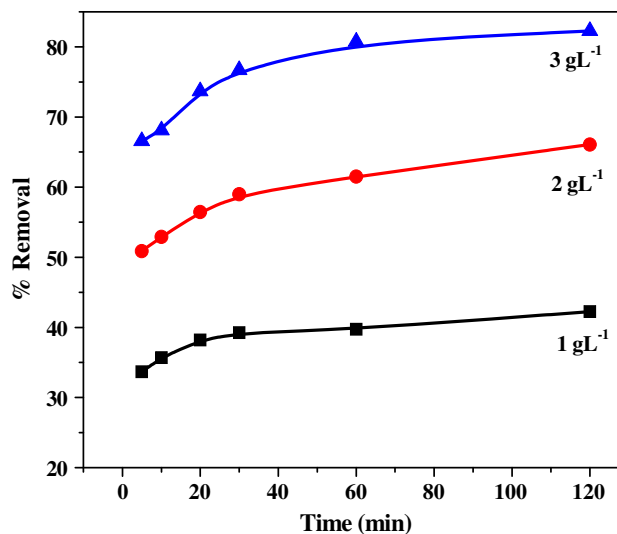**Fig. 3** Effect of adsorbent dose on percentage removal of Cr(VI) on activated carbon ($C_0 = 60$ mg L^{-1}, T = 303 K)

Fig. 2 Effect of initial metal ion concentration on maximum metal ion uptake and percentage removal of Cr(VI) on activated carbon (w = 1 g L^{-1}, T = 303 K, time = 120 min)

Fig. 4 Effect of contact time on Cr(VI)/activated carbon adsorption (w = 1 g L^{-1}, C_0 = 40–100 mg L^{-1}, T = 303 K)
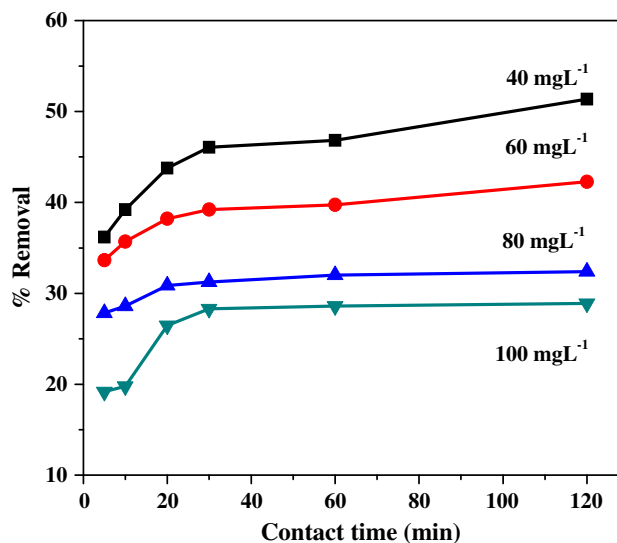
concentration of Cr(VI) from 20 to 100 mg L^{-1}. When concentration increases there is an increase in number of Cr(VI) ions. The large number of ions completely occupied the active sites of the surface of the adsorbent which is not possible in a lower concentration. Hence there is an increase in amount of maximum metal ion uptake.

3.5.2 Effect of adsorbent dose

Figure 3 shows the effect of adsorbent dose on the removal of Cr(VI). This effect was studied by varying the adsorbent dose from 1 to 3 g L^{-1}. The experiments were carried out at a pH 4.8, 60 mg L^{-1} initial dye concentration and at a temperature of 303 K. The removal of Cr(VI) was increased from 42.26 to 82.27 % with the increase of adsorbent dose. When we increase the adsorbent dose,

there is an increase in surface area and more active sites are available for adsorption. This is responsible for the increase in Cr(VI) removal with increase in adsorbent dose.

3.5.3 Effect of contact time
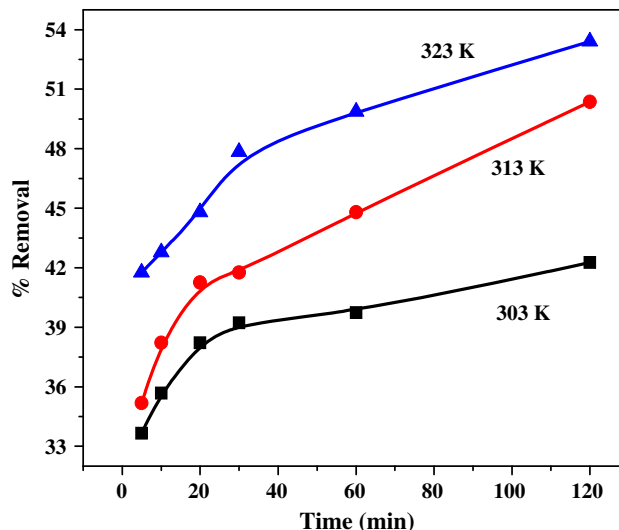
The adsorption experiments were carried out for different contact times with initial metal ion concentration of (40–100) mg L^{-1} and using a fixed amount of adsorbent dose (1 g L^{-1}). It is shown in Fig. 4. From the figure it is clear that the percentage removal of Cr(VI) increases with increasing contact time. Time required to attain the equilibrium was 120 min.
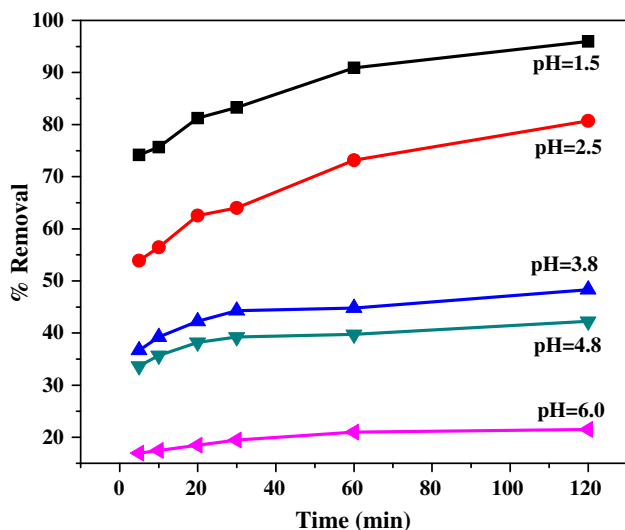
Fig. 5 Plot of time versus % removal of Cr(VI) over activated carbon at different pH ($C_0 = 60$ mg L^{-1}, w = 1 g L^{-1}, T = 303 K)

Fig. 6 Effect of temperature on percentage removal of Cr(VI) on activated carbon (w = 1 g L^{-1}, $C_0 = 60$ mg L^{-1})

3.5.4 Effect of pH

The pH of the aqueous solution is an important controlling parameter in the metal adsorption process as the charge density of the adsorbent surface and metallic species depend on pH. The effect of pH on removal of Cr(VI) is shown in Fig. 5. The initial pH of the solution was adjusted to the required value by using 0.1 M NaOH or HCl solution. The experiment was carried out by using Cr(VI) solution of concentration 60 mg L^{-1}, adsorbent dose 1 g L^{-1} and at temperature 303 K. Percentage removal of Cr(VI) decreases from 95.95 to 21.5 % when pH increases from 1.5 to 6. Same trend was observed for adsorption capacity also. With increase in pH from 1.5 to 6 adsorption capacity decreases from 57.57 to 12.9 mg g^{-1} (Figure S4, Supporting information). The adsorption capacity at pH 4.8 (normal pH of the dichromate solution) was found to be 25.36 mg g^{-1}. Surface of activated carbon contains number of functional groups and the pH dependence of Cr(VI) adsorption can be related to the type and ionic state of these functional groups. It is well known that the dominant form of Cr(VI) at lower pH is $HCrO_4^{-}$. Increasing the pH will shift the concentration of $HCrO_4^{-}$ to other forms, CrO_4^{2-} and $Cr_2O_7^{2-}$. At low pH a large number of H$^+$ ions are present which may increase the positive charge density on the adsorbent surface resulting less hindrance to the diffusion of chromate ions. Hence $HCrO_4^{-}$ is adsorbed preferentially on the surface of the carbon. The decrease in removal at higher pH may be due to abundance of OH$^-$ ions which causes the increase in negative charge density on the surface of activated carbon [33]. Or we can say that more functional groups carrying positive charge would be exposed at low pH. High adsorption of Cr(VI) at low pH can be attributed to the binding of negatively charged species through electrostatic attraction to those positively charged functional groups on the surface of activated carbon. At higher pH there is an electrostatic repulsion between the adsorbent surface and the chromate anions as more functional groups carrying negative charge are there on the carbon surface [34]. Hence a decrease in percentage removal of Cr(VI) was observed at higher pH.

3.5.5 Effect of temperature

To study the effect of temperature on removal of Cr(VI) the adsorption experiments were carried out at three different temperatures (303, 313 and 323 K). Figure 6 illustrates the effect of temperature on removal of Cr(VI). With increase in temperature the percentage removal of Cr(VI) increases. The percentage removal increases from 42.26 to 53.4 % when the temperature was increased from 303 to 323 K. As temperature increases the mobility of the Cr(VI) ions also increases due to which the interaction between the Cr(VI) ions and the active sites increases resulting more adsorption of the metal ions to the adsorbent surface. Increase in percentage removal with increasing temperature confirms the endothermic nature of the adsorption process.

3.6 Adsorption isotherms

To model the adsorption behavior and calculate the adsorption capacity of the activated carbon, adsorption isotherms were studied. The Langmuir, Freundlich and Tempkin isotherm models were examined to describe the adsorption equilibrium. Linear regression was used to determine the best fitting model.
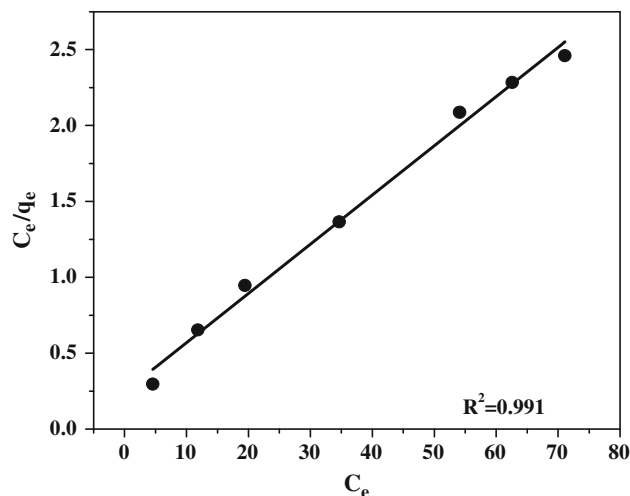
Fig. 7 Langmuir adsorption isotherm for removal of Cr(VI) by activated carbon (w = 1 g L^{-1}, T = 303 K)

3.6.1 Langmuir isotherm

According to Langmuir adsorption isotherm model, adsorption occurs uniformly on the active sites of the adsorbent surface. Once an adsorbate occupies an active site, no further adsorption can take place at that site. The Langmuir adsorption equation is [35, 36]:

$$\frac{C_e}{q_e} = \frac{1}{Q_0 b} + \frac{C_e}{Q_0} \tag{5}$$

where, q_e is the amount of Cr(VI) adsorbed (mg g^{-1}) at equilibrium. C_e is the equilibrium solution concentration (mg L^{-1}). Q_0 and b, the Langmuir constants represent the maximum adsorption capacity (mg g^{-1}) and energy of adsorption respectively. A plot of C_e/q_e versus C_e should be a straight line with slope $1/Q_0$ and intercept $1/Q_0 b$. Langmuir plot for adsorption of Cr(VI) on activated carbon is shown in Fig. 7.

The essential characteristics of the Langmuir isotherm can be made on the basis of a dimensionless equilibrium parameter, R_L, also known as separation factor is given by [36]:

$$R_L = \frac{1}{1 + bC_0} \tag{6}$$

where C_0 is the initial Cr(VI) concentration and b is the Langmuir constant. If the value of R_L is in between 0 and 1 the adsorption is favorable. If it is more than 1 then the adsorption is not favorable.

The Langmuir plot has a good linearity having the correlation coefficient (R^2) value 0.991. The adsorption capacity (Q_0) and energy of adsorption (b) calculated from the slope and intercept of the Langmuir plot are found to be 30.8 mg g^{-1} and 0.13 L mg^{-1} respectively. The separation

factor R_L has the value between 0 and 1 indicating the adsorption of Cr(VI) on the activated carbon prepared from matured tea leaves is a favorable one.

3.6.2 Freundlich isotherm

The Freundlich isotherm model is based on the assumption that the adsorbate absorbs onto the heterogeneous surface of an adsorbent [36, 37]. This model is expressed by the following equation:

$$\log q_e = \log K_F + \frac{1}{n} \log C_e \tag{7}$$

where q_e is the amount adsorbed (mg g^{-1}), C_e is the equilibrium concentration of Cr(VI) solution (mg L^{-1}), K_F and n are the Freundlich constants which represent adsorption capacity and adsorption intensity respectively.

When $\log q_e$ was plotted against $\log C_e$, a straight line with slope $1/n$ and intercept $\log K_F$ was obtained (Figure S5, Supporting Information). 'K_F' and 'n' calculated from the plot were 10.63 and 4.34 respectively. The value of 'n' in between 2 and 10 indicates favorable adsorption [38]. The 'n' value of 4.34 suggests that the activated carbon is an effective adsorbent for adsorption of Cr(VI).

3.6.3 Temkin adsorption isotherm

The assumption of Temkin adsorption isotherm is that with coverage of the molecular layer due to adsorbent adsorbate interaction the heat of adsorption of all the molecules decreases. Another assumption of this model is the characterization of adsorption by a uniform distribution of binding energies up to some maximum value [39, 40].

The Temkin isotherm can be written as

$$q_e = \frac{RT}{b} \ln(K_T C_e) \tag{8}$$

where, b is the Temkin constant related to heat of adsorption (J mol^{-1}). The linearized form of the equation is:

$$q_e = B_1 \ln K_T + B_1 \ln C_e \tag{9}$$

where, $B_1 = \frac{RT}{b}$, K_T is the Temkin isotherm energy constant (L mg^{-1}). When we plotted q_e against $\ln C_e$, a straight line with R^2 value 0.958 was obtained (Figure S6, Supporting Information). From the slope and intercept of the graph, B_1 and K_T values were calculated. As the plot for Temkin adsorption isotherm is found to be linear with a high correlation coefficient value, we can say that the adsorption of Cr(VI) onto the activated carbon is a chemisorptions process.

All the calculated values of Langmuir, Freundlich and Temkin constants are summarized in Table 2. From these

Table 2 Langmuir, Freundlich and Temkin constants for the removal of Cr(VI) over activated carbon

Langmuir isotherm			Freundlich isotherm			Temkin isotherm		
Constants		R^2	Constants		R^2	Constants		R^2
b (L mg^{-1})	Q$_0$ (mg g^{-1})		n	K$_F$ (mg g^{-1})		B$_1$	K$_T$ (L mg^{-1})	
0.13	30.8	0.991	4.34	10.63	0.977	0.196	0.0017	0.958

Table 3 Langmuir separation factor values obtained for different initial concentrations at 303 K

Initial concentration (mg L^{-1})	R$_L$ values
40	0.159
60	0.112
80	0.086
100	0.07

values it is clear that Langmuir Isotherm ($R^2 = 0.991$) model is the best fitted model for Cr(VI) adsorption on activated carbon. Values of Langmuir separation factor (R_L) are listed in Table 3.

3.7 Adsorption kinetics

The adsorption process of Cr(VI) onto activated carbon was investigated by the well known kinetic models such as the linearized form of pseudo first order, pseudo second order and intra particle diffusion model. The pseudo first order kinetic model was given by Lagergren and the linearized form of the equation is [41]:

$$\log(q_e - q_t) = \log q_e - \frac{k_1}{2.303}t \tag{10}$$

where q_t (mg g^{-1}) and q_e (mg g^{-1}) are the amount of metal adsorbed at time t and equilibrium respectively, k_1 is the rate constant of pseudo first order adsorption (min^{-1}).

Plot of log ($q_e - q_t$) versus time (t) did not give a straight line. This shows that adsorption of Cr(VI) on the activated carbon is not a first order reaction.

The adsorption kinetics can be described by pseudo second order model. The linear form of the pseudo second order rate equation is as follows: [42, 43]

$$\frac{t}{q_t} = \frac{1}{k_2 q_e^2} + \frac{t}{q_e} \tag{11}$$

where q_t (mg g^{-1}) and q_e (mg g^{-1}) are the amount of metal adsorbed at time t and equilibrium respectively, k_2 is the equilibrium rate constant of pseudo second order adsorption (g mg^{-1} min^{-1}).The values of q_e and k_2 were determined from the slope and intercept of the linear plot of t/q_t versus time (t) (Fig. 8). The results are shown in Table 4 along with the corresponding correlation coefficients. This results give a good agreement between the experimental adsorption capacity [q_e(exp)] values that with the
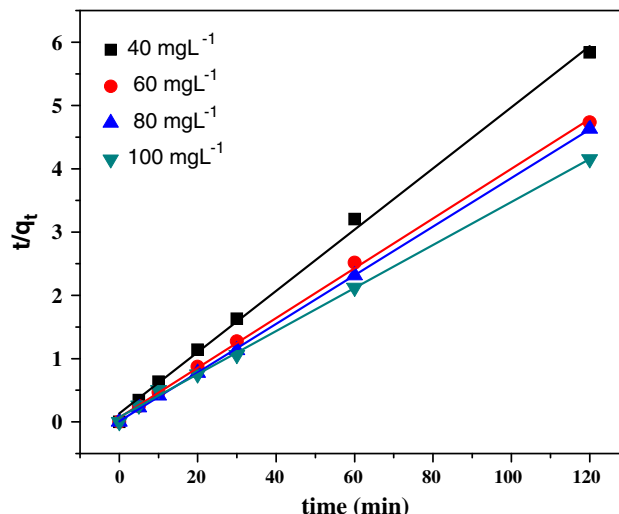
Fig. 8 Pseudo-second-order kinetic plot for removal of Cr(VI) by activated carbon (w = 1 g L^{-1}, T = 303 K)

calculated values [q_e (cal)]. The very high correlation coefficient values ($R^2 > 0.99$) also indicate that the pseudo second order kinetic model is well applicable to describe the adsorption of Cr(VI) on the activated carbon.

3.8 Intra particle diffusion

The intra particle diffusion model was also used to study the diffusion mechanism. This model is expressed as [28, 44]:

$$q_t = k_{id}t^{0.5} + C \tag{12}$$

where k_{id} is the intra particle diffusion rate constant (mg g^{-1} min$^{-0.5}$), C is the constant characterizing boundary layer thickness. Larger the C value (intercept) the greater is the boundary layer effect. When the adsorption mechanism follows intra particle diffusion process, the plot of q_t versus $t^{0.5}$ should be a straight line with slope k_{id} and intercept C. Figure (S7, Supporting Information) shows the plots of q_t versus $t^{0.5}$ for the adsorption of Cr(VI) onto the activated carbon. The calculated values of intra particle diffusion constants are shown in Table 5. The linearity of the plots indicates that intra particle diffusion plays a significant role in the adsorption of Cr(VI) by the activated carbon. Deviation of the straight line from the origin may

Table 4 Pseudo second order kinetic constants for removal of Cr(VI) over activated carbon

T K	C_0 mg L^{-1}	k_2 g mg^{-1} min^{-1}	q_e(cal) mg g^{-1}	q_e(exp) mg g^{-1}	R^2
303	40	0.017	20.67	20.55	0.997
	60	0.022	25.44	25.36	0.999
	80	0.149	26.01	25.91	0.999
	100	0.015	29.41	28.89	0.999

Table 5 Intra particle diffusion constants for different adsorbent dosage at 303 K

Adsorbent dose g L^{-1}	k_{id} mg g^{-1} $min^{-0.5}$	C	R^2
1	0.5372	19.83	0.86
2	0.5147	14.42	0.96
3	0.3781	12.79	0.86

be due to the reason that pore diffusion is not the rate controlling step in this process. The adsorption process involves two steps- adsorption on the external surface and diffusion into the interior surface [45]. These steps are indistinguishable from one another and we can say that the intra particle diffusion is prominent from the beginning of adsorbate-adsorbent interaction.

3.9 Thermodynamic study of adsorption

To describe thermodynamic behavior of the adsorption of Cr(VI) onto the activated carbon, thermodynamic parameters, the change in free energy, (ΔG^0), enthalpy ΔH^0 and entropy (ΔS^0)were calculated. The relation between ΔG^0, ΔH^0 and ΔS^0 is as follows:

$$\Delta G^0 = \Delta H^0 - T\Delta S^0 \tag{13}$$

The adsorption equilibrium constant K_c was calculated by the ratio of amount of adsorbate adsorbed (q_e) to the amount remaining in the solution (C_e):

$$K_c = \frac{q_e}{C_e} \tag{14}$$

Gibbs free energy was calculated by the following equation using K_c:

$$\Delta G^0 = -RT \ln K_c \tag{15}$$

Based on the above equations the following van't Hoff equation can be derived:

$$\ln K_c = \frac{\Delta S^0}{R} - \frac{\Delta H^0}{RT} \tag{16}$$

ΔH^0 and ΔS^0 were obtained from the slope and intercept of the plot of ln K_c versus 1/T. The van't Hoff plot for the

Table 6 Thermodynamic parameters for Cr(VI)/activated carbon adsorption

Temperature K	ΔH^0 KJ mol^{-1}	ΔG^0 KJ mol^{-1}	ΔS^0 J mol^{-1} K^{-1}
303		−0.145	
313	28.6	−1.09	94.87
323		−2.04	

Table 7 Adsorption capacity of various adsorbents for Cr(VI) adsorption

Adsorbent	Q_0 (mg g^{-1})	pH	Reference
Matured tea leaves AC	30.8	4.8	This study
Coconut tree sawdust AC	3.46	3	[2]
Carbonaceous adsorbent from waste tires (TAC)	58.5	2	[17]
Carbonaceous adsorbent from sawdust (SPC)	2.3		
Carbon, F-400	53.2		
Wool	41.15	2	[18]
Olive cake	33.44		
Sawdust	15.823		
Pine needles	21.5		
Almond	10.616		
Coal	6.78		
Cactus	7.082		
Terminalia arjunanuts AC	28.43	1	[46]
Graciliriaedulis AC	29.89	1	[47]
OS-Sulfuric acid AC	71	1.5	[48]
Wood apple shell AC	13.74	2	[49]
Coconut shell AC	6.0	3–4	[50]
Wood AC	5.1	2	
Dust coal AC	4.4	3–4	
Hazelnut shell AC	17.7	2	[51]

adsorption of Cr(VI) onto activated carbon is shown in Figure (S8, Supporting Information) and the thermodynamic parameters calculated are summarized in Table 6. The positive value of ΔH^0 and negative values of ΔG^0 confirm the endothermic and spontaneous nature of the adsorption process.

4 Comparison of adsorption capacity with some other adsorbents

The adsorption capacity of activated carbon derived from matured tea leaves was compared with various adsorbents

that were used by other researchers [2, 17, 18, 46–51] which are shown in Table 7. From the table it is clear that most of the studies are performed at very low pH value. The as synthesized porous carbon shows very good adsorption capacity for a wide range of pH (1.5–4.8) value with highest a value of 57.57 at pH 1.5 for a solution of concentration of 60 mg L^{-1}. The adsorption capacity calculated from Langmuir isotherm at pH 4.8 (normal pH of the dichromate solution) was found to be 30.8 mg g^{-1} (Table 7).

5 Conclusion

In conclusion, activated carbon prepared from matured tea leaves acts as an excellent adsorbent material for removal of Cr(VI) from wastewater. Matured tea leaves are abundantly found waste material and hence the activated carbon prepared is expected to be of low cost. The adsorption capacity of the material is found to be very good in a wide range of pH (1.5–4.8) value. The adsorption capacity as calculated from Langmuir isotherm was found to be 30.8 mg g^{-1} at pH 4.8 and temperature 303 K. The kinetic studies showed that pseudo second order rate equation can provide a better description of the adsorption process. Langmuir, Freundlich and Temkin isotherms were used to study the adsorption process. Langmuir isotherm was best fitted with better correlation coefficient than other two models. Adsorption kinetics of Cr(VI) was best described by the pseudo second order kinetic equation. Adsorption capacity of Cr(VI) was increased with increase in temperature which reveals the endothermic nature of the adsorption process which was further confirmed by the thermodynamic parameters.

References

1. S. Chen, Q. Yue, B. Gao, Q. Li, X. Xu, K. Fu, Bioresour. Technol. **113**, 114–120 (2012)
2. K. Selvi, S. Pattabhi, K. Kadirvelu, Bioresour. Technol. **80**, 87–89 (2001)
3. V.K. Gupta, A. Rastogi, A. Nayak, J. Colloid Interface Sci. **342**, 135–141 (2010)
4. V.K. Gupta, I. Ali, T.A. Saleh, A. Nayak, S. Agarwal, RSC Adv. **2**, 6380–6388 (2012)
5. H. Shaalan, M. Sorour, S. Tewfik, Desalination **14**, 315–324 (2001)
6. D. Mohan, C.U. Pittman Jr, J. Hazard. Mater. **B137**, 762–811 (2006)
7. E. Salazar, M.I. Ortiz, A.M. Urtiaga, J.A. Irabien, Ind. Eng. Chem. Res. **31**, 1516–1522 (1992)
8. D. Petruzzelli, J.R. Passino, G. Tiravantit, Ind. Eng. Chem. Res. **34**, 2612–2617 (1996)
9. D. Mohan, K.P. Singh, V.K. Singh, Ind. Eng. Chem. Res. **44**, 1027–1042 (2005)
10. T.A. Saleh, V.K. Gupta, Environ. Sci. Pollut. Res. **19**, 1224–1228 (2012)
11. V.K. Gupta, S.K. Srivastava, D. Mohan, S. Sharma, Waste Manag. **17**, 517–522 (1998)
12. V.K. Gupta, R. Jain, A. Mittal, T.A. Saleh, A. Nayak, S. Agarwal, S. Sikarwar, Mater. Sci. Eng. C **32**, 12–17 (2012)
13. V.K. Gupta, R. Jain, A. Nayak, S. Agarwal, M. Shrivastava, Mater. Sci. Eng. C **31**, 1062–1067 (2011)
14. T.A. Saleh, V.K. Gupta, J. Colloid Interface Sci. **371**, 101–106 (2012)
15. S. Karthikeyan, V.K. Gupta, R. Boopathy, A. Titus, G. Sekaran, J. Mol. Liq. **173**, 153–163 (2012)
16. J.M. Dias, M.C.M. Alvim-Ferraz, M.F. Almeida, J. Rivera-Utrillab, M. Sánchez-Polo, J. Environ. Manag. **85**, 833–846 (2007)
17. N.K. Hamadi, X.D. Chen, M.M. Farid, M.G.Q. Lu, Chem. Eng. J. **84**, 95–105 (2001)
18. M. Dakiky, A. Khami, A. Manassra, M. Mer'eb, Adv. Environ. Res. **6**, 533–540 (2002)
19. M. Kobya, Bioresour. Technol. **91**, 317–321 (2004)
20. A. Mittal, D. Kaur, A. Malviya, J. Mittal, V.K. Gupta, J. Colloid Interface Sci. **337**, 345–354 (2009)
21. A. Mittal, J. Mittal, A. Malviya, V.K. Gupta, J. Colloid Interface Sci. **340**, 16–26 (2009)
22. A. Mittal, J. Mittal, A. Malviya, V.K. Gupta, J. Colloid Interface Sci. **344**, 497–507 (2010)
23. A. Mittal, J. Mittal, A. Malviya, D. Kaur, V.K. Gupta, J. Colloid Interface Sci. **342**, 518–527 (2010)
24. A.K. Jain, V.K. Gupta, A. Bhatnagar, Suhas, Sep. Sci. Technol. **38**, 463–481 (2003)
25. V.K. Gupta, A. Nayak, Chem. Eng. J. **180**, 81–90 (2012)
26. H. Khani, M.K. Rofouei, P. Arab, V.K. Gupta, Z. Vafaei, J. Hazard. Mater. **183**, 402–409 (2010)
27. V.K. Gupta, S. Agarwal, T.A. Saleh, J. Hazard. Mater. **185**, 17–23 (2011)
28. L.J. Kennedy, J.J. Vijaya, K. Kayalvizhi, G. Sekaran, Chem. Eng. J. **132**, 279–287 (2007)
29. L. Borah, K.K. Senapati, C. Borgohain, S. Sarma, S. Roy, P. Phukan, J. Porous Mater. **19**, 767–774 (2012)
30. M.T. Uddin, M.A. Islam, S. Mahmud, M. Rukanuzzaman, J. Hazard. Mater. **164**, 53–60 (2009)
31. L. Khenniche, F. Benissad-Aissani, J. Chem. Eng. Data **55**, 4677–4686 (2010)
32. J. Anandkumar, B. Mandal, J. Hazard. Mater. **168**, 633–640 (2009)
33. H. Demiral, I. Demiral, F. Tumsek, B. Karabacakoglu, Chem. Eng. J. **144**, 188–196 (2008)
34. E. Malkoc, Y. Nuhoglu, Sep. Purif. Technol. **54**, 291–298 (2007)
35. I. Langmuir, J. Am. Chem. Soc. **38**, 2221–2295 (1916)
36. E. Oguz, Colloids Surf. A **252**, 121–128 (2005)
37. H.M.F. Freundlich, Z. Uber, Z. Phys. Chem. **57A**, 385–470 (1906)
38. G. McKay, M.S. Otterburn, A.G. Sweeney, Water Res. **14**, 15–20 (1980)
39. Ö. Özcan, İ. İnci, Y.S. Aşçi, J. Chem. Eng. Data **58**, 583–587 (2013)
40. İ. İnci, Ş.S. Bayazit, Y.S. Aşçi, J. Chem. Eng. Data **56**, 4449–4453 (2011)
41. S. Lagergren, K. Sven, Vetenskapsakad. Handl. **24**, 1–39 (1898)
42. Y.S. Ho, G. Mckay, Process Biochem. **34**, 451–465 (1999)
43. Y.S. Ho, J. Hazard. Mater. **136**, 681–689 (2006)

44. B.H. Hameed, D.K. Mahmoud, A.L. Ahmad, J. Hazard. Mater. **158**, 65–72 (2008)
45. K.G. Bhattacharyya, A. Sharma, Dyes Pigm. **65**, 51–59 (2005)
46. K. Mohanty, M. Jha, B.C. Meikap, M.N. Biswas, Chem. Eng. Sci. **60**, 3049–3059 (2005)
47. S.T. Natarajan, R. Jayaraj, P.J. Thanaraj, P.M.D. Prasath, J. Chem. Pharm. Res. **3**, 595–604 (2011)
48. A.A. Attia, S.A. Khedr, S.A. Elkholy, Braz. J. Chem. Eng. **27**, 183–193 (2010)
49. A.S. Sartape, P.D. Raut, S.S. Kolekar, Adsorpt. Sci. Technol. **28**, 547–560 (2010)
50. V. Selomulya, R.Amal Meeyoo, J. Chem. Technol. Biotechnol. **74**, 111–122 (1999)
51. G. Cimino, A. Passerini, G. Toscano, Water Res. **34**, 2955–2962 (2000)